

LoFT: Parameter-Efficient Fine-Tuning for Long-tailed Semi-Supervised Learning in Open-World Scenarios

Zhiyuan Huang, Jiahao Chen, Yurou Liu, Bing Su

Renmin University of China
nicelemon666@gmail.com

Abstract

Long-tailed learning has garnered increasing attention due to its wide applicability in real-world scenarios. Among existing approaches, Long-Tailed Semi-Supervised Learning (LTSSL) has emerged as an effective solution by incorporating a large amount of unlabeled data into the imbalanced labeled dataset. However, most prior LTSSL methods are designed to train models from scratch, which often leads to issues such as overconfidence and low-quality pseudolabels. To address these challenges, we extend LTSSL into the foundation model fine-tuning paradigm and propose a novel framework: LoFT (Long-tailed semi-supervised learning via parameter-efficient Fine-Tuning). We demonstrate that fine-tuned foundation models can generate more reliable pseudolabels, thereby benefiting imbalanced learning. Furthermore, we explore a more practical setting by investigating semi-supervised learning under open-world conditions, where the unlabeled data may include out-of-distribution (OOD) samples. To handle this problem, we propose LoFT-OW (LoFT under Open-World scenarios) to improve the discriminative ability. Experimental results on multiple benchmarks demonstrate that our method achieves superior performance compared to previous approaches, even when utilizing only 1% of the unlabeled data compared with previous works.

Introduction

Real-world data often follows a long-tailed or imbalanced distribution, where a small number of head classes dominate the majority of samples, while the remaining tail classes are represented by only a limited number of instances (Cui et al. 2019). This imbalance poses significant challenges for model training, particularly in achieving satisfactory performance on tail classes. To address this issue, Long-Tailed Semi-Supervised Learning (LTSSL) has emerged as an effective solution by incorporating a large amount of unlabeled data into the imbalanced labeled dataset (Wei et al. 2021; Wei and Gan 2023). The basic idea of LTSSL is to generate pseudo-labels for unlabeled data and select high-confidence samples to guide model training (Ouali, Hudelot, and Tami 2020). While the current methods have achieved notable success and demonstrated promising results, they still face dilemmas hindering further improvement.

Previous LTSSL approaches typically rely on training Convolutional Neural Networks (CNNs) from scratch (Wei

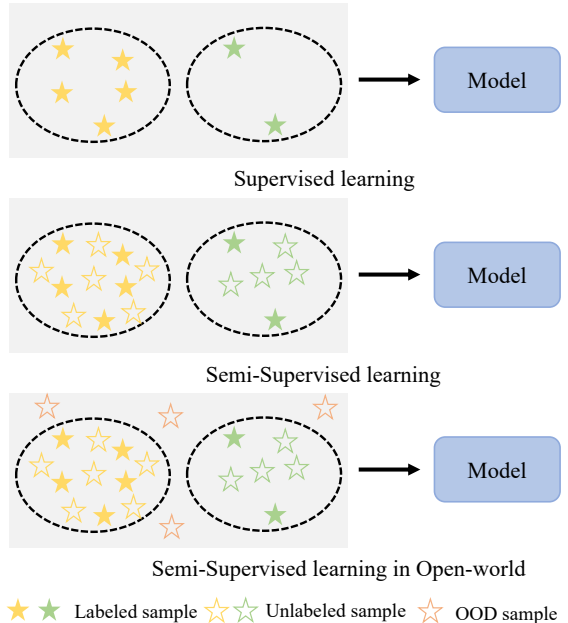


Figure 1: Differences among supervised learning, semi-supervised learning, and semi-supervised learning in open-world scenarios. Pentagrams in yellow and green denote samples of head classes and tail classes, respectively.

et al. 2021), which presents several challenges. First, CNNs are known to be overconfident (Guo et al. 2017), often assigning high-confidence scores to incorrect predictions. Although methods like FixMatch (Sohn et al. 2020) employ a “weak-to-strong” pipeline, using weakly augmented samples to determine labels and strong augmented samples to determine the logits, this overconfidence issue persists, especially for tail classes, as shown in Fig. 2. Second, in the early training stages, the model produces unreliable predictions, resulting in low-quality pseudo-labels. As a result, current LTSSL approaches often require more training iterations and carefully designed strategies to dynamically manage the use of unlabeled data (Wei and Gan 2023). Both of the dilemmas limit the application of LTSSL.

To alleviate the above issues, we propose a novel and effective *Long-tailed semi-supervised learning via parameter*

efficient Fine-Tuning (LoFT) framework. For details, LoFT is built upon transformer-based foundation models, e.g., vision transformer (ViT) (Dosovitskiy et al. 2020), which are pre-trained on a large-scale dataset and fine-tuned via Parameter-Efficient Fine-Tuning (PEFT). We find that our LoFT can well tackle the above issues in existing methods as aforementioned. Firstly, the model fine-tuned via LoFT is native well calibrated for both head classes and tail classes, as shown in Fig. 2. Compared with previous works, using a fixed threshold to filter reliable samples, LoFT can decrease the interference of samples assigning erroneous pseudo-labels. Second, foundation models have a high generalization ability for downstream tasks, which can reduce training time and reduce the impact of low model discrimination ability in the early stage of training, thereby reducing the impact of pseudo-label uncertainty.

Beyond the traditional LTSSL setting, we also explore a more challenging and realistic scenario, referred to as Long-tailed Semi-Supervised Learning in Open-World Scenarios. The key distinction lies in the composition of the unlabeled data: unlike standard LTSSL, the unlabeled set in open-world scenarios may contain a substantial proportion of out-of-distribution (OOD) samples that do not belong to any of the labeled classes, as shown in Fig. 1. For example, when training a wildlife classification model using images from known species, the unlabeled data may include rare or unknown animals not present in the labeled dataset, introducing additional complexity and ambiguity into the training process. If existing LTSSL methods are directly applied in such scenarios, OOD samples may be erroneously assigned in-distribution labels, thereby misleading the learning process. Furthermore, models trained from scratch generally lack the capacity to effectively identify or reject these OOD samples (Hendrycks and Gimpel 2016). To address this issue, our proposed LoFT-OW (LoFT under Open-World scenarios) framework inherently incorporates an OOD detection mechanism that enables the model to natively filter out irrelevant samples, as evidenced by the results in Tab. 1. By mitigating the negative impact of OOD instances, LoFT facilitates more discriminative representation learning and enhances robustness under diverse data conditions.

Our contributions can be summarized as follows:

- We address the LTSSL problem and propose LoFT, a novel framework that leverages Parameter-Efficient Fine-Tuning (PEFT) of transformer-based foundation models (e.g., ViT). Through comprehensive experiments, we analyze the confidence behavior of LoFT and observe that it is inherently well-calibrated. We further demonstrate that this property can be effectively utilized to improve the quality of pseudo-labels.
- We extend LTSSL to a more realistic Open-World Scenario, named LoFT-OW, where unlabeled data may contain OOD samples. LoFT incorporates a built-in OOD detection mechanism, filtering out irrelevant samples and improving model robustness and representation learning in diverse real-world data conditions.
- We conduct experiments on traditional LTSSL benchmarks, including CIFAR-LT and ImageNet127, and ob-

serve that LoFT achieves competitive performance. Furthermore, LoFT achieves superior performance in the more challenging open-world scenarios, outperforming previous methods even when using only 1% of the unlabeled data compared with previous works, highlighting its strong discriminative capability.

Related work

Long-tailed semi-supervised learning Long-Tailed Semi-Supervised Learning (Peng et al. 2023; Hou and Jia 2025; Wei et al. 2021) (LTSSL) aims to improve the performance of models trained on long-tailed labeled data by leveraging additional unlabeled data. The basic idea is to generate pseudolabels for the unlabeled samples and incorporate them into the training process. CReST (Wei et al. 2021) observes that models trained under imbalanced distributions can still generate high-precision pseudolabels for tail classes. Based on this insight, it proposes the class-rebalancing self-training framework to improve performance. In (Wei and Gan 2023), the authors relax the assumption of consistent class distributions between labeled and unlabeled data and introduce ACR, a method that dynamically refines pseudo-labels by estimating the true class distribution of unlabeled data under a unified formulation. ADELLO (Sanchez Aimar et al. 2023) presents FlexDA, a dynamic logit adjustment and distillation-based framework that enhances calibration and achieves strong performance in LTSSL settings. Recently, foundation models (Radford et al. 2021), pre-trained on large-scale datasets, have demonstrated strong generalization capabilities across a variety of downstream tasks, including those with long-tailed distributions (Shi et al. 2024; Tian et al. 2022; Dong et al. 2022). However, how to effectively leverage foundation models to benefit LTSSL remains an open and underexplored research direction. In this paper, we aim to address this challenge and propose LoFT, a novel framework designed to integrate the strengths of foundation models into the LTSSL paradigm.

Long-tailed Confidence calibration Confidence calibration aims to align the predicted confidence scores with the true accuracy, which is important for safety measurement, out-of-distribution detection (Liu et al. 2024). Prior studies have shown that modern CNNs tend to be overconfident (Tomani et al. 2021; Guo et al. 2017), particularly under long-tailed distributions (Zhong et al. 2021). MiSLAS (Zhong et al. 2021) addresses this issue by introducing a two-stage training pipeline that incorporates three key techniques: mixup (Zhang et al. 2017) pre-training, label-aware smoothing, and batch normalization () shifting. These techniques collectively enhance the model’s calibration capability. UniMix (Xu, Chai, and Yuan 2021) extends the mixup strategy to imbalanced scenarios by adopting an advanced mixing factor and a sampling strategy that favors minority classes, thereby improving calibration performance under long-tailed distributions. Recently, adapting foundation models to imbalanced learning has attracted increasing attention. However, the issue of confidence calibration in this setting remains largely underexplored. As previously

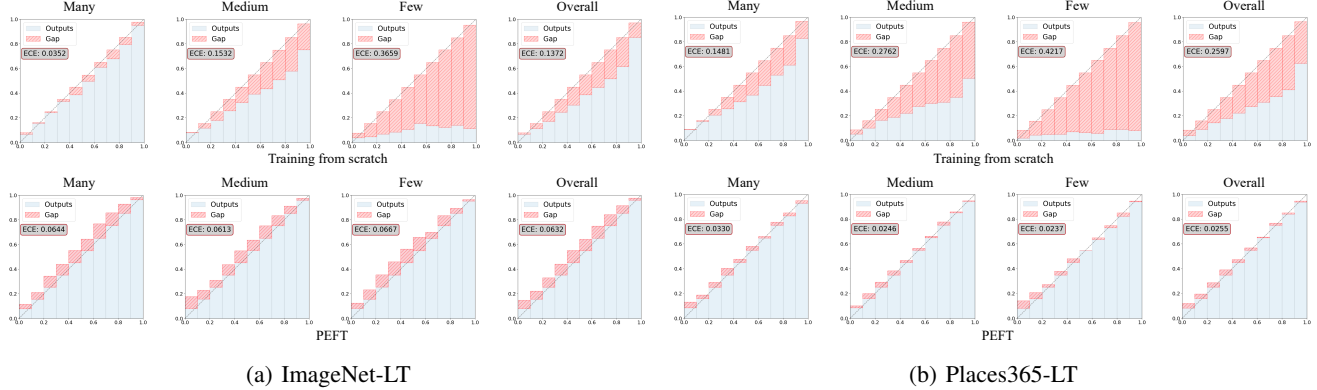


Figure 2: The reliability diagrams on (a) ImageNet-LT and (b) Places365-LT based on training from scratch and PEFT, respectively. The horizontal axis represents confidence, and the vertical axis represents accuracy.

discussed, a well-calibrated model is crucial for generating high quality pseudo-labels, which are essential for effective semi-supervised learning. In this work, we investigate confidence calibration within the context of LTSSL to further enhance performance under long-tailed distributions.

Preliminary

Notation Our target is to solve a K -way classification problem, where each input sample $\mathbf{x} \in \mathcal{X}$ is associated with a label $y \in \mathcal{Y} = [K] = \{1, \dots, K\}$, with \mathcal{X} and \mathcal{Y} denoting the input and output spaces, respectively. In the context of LTSSL, we are given a labeled training set $\mathcal{D}_S = \{(\mathbf{x}_i, y_i)\}_{i=1}^{N_S}$ and an unlabeled set $\mathcal{D}_U = \{\mathbf{x}_i\}_{i=1}^{N_U}$. The labeled set \mathcal{D}_S follows a long-tailed distribution, i.e., the class priors satisfy $\mathbb{P}_S(Y = 1) \neq \mathbb{P}_S(Y = 2) \neq \dots \neq \mathbb{P}_S(Y = K)$, where $\mathbb{P}_S(Y)$ denotes the class distribution in \mathcal{D}_S . In contrast, we impose no assumptions on the class distribution of the unlabeled set \mathcal{D}_U ; it may or may not follow the same distribution as \mathcal{D}_S . For the test set $\mathcal{D}_T = \{(\mathbf{x}_i, y_i)\}_{i=1}^{N_T}$, we assume an almost uniform class distribution, i.e., $\mathbb{P}_T(Y = k) \approx 1/K$ for all $k \in [K]$. Our target is to learn a hypothesis $f : \mathcal{X} \rightarrow \mathbb{R}^K$ that estimates $\mathbb{P}_S(Y = y \mid \mathbf{x})$ by leveraging both \mathcal{D}_S and \mathcal{D}_U , thereby achieving generalization on the balanced test distribution.

Zero-shot classification We adopt CLIP (Radford et al. 2021) as the zero-shot classification backbone. CLIP consists of an image encoder $\phi_I : \mathcal{X} \rightarrow \mathbb{R}^d$ and a text encoder $\phi_T : \mathcal{T} \rightarrow \mathbb{R}^d$, which project visual and textual inputs into a shared embedding space. To perform classification, we define a set of prompt-based textual queries $\{t_k\}_{k=1}^K$ for each class $k \in [K]$, such as “*a photo of a [Class]*”. These are encoded as class prototypes $\mathbf{w}_k = \phi_T(t_k)$.

Given an input image $\mathbf{x} \in \mathcal{X}$, its embedding is obtained as $\mathbf{z}_x = \phi_I(\mathbf{x})$. CLIP computes the cosine similarity between \mathbf{z}_x and each class prototype:

$$\text{sim}(\mathbf{z}_x, \mathbf{w}_k) = \frac{\mathbf{z}_x^\top \mathbf{w}_k}{\|\mathbf{z}_x\| \cdot \|\mathbf{w}_k\|}.$$

The final prediction is made by applying a softmax over the

similarity scores:

$$f_{\mathbf{z}_x}(\mathbf{x}) = \text{softmax}([\text{sim}(\mathbf{z}_x, \mathbf{w}_1), \dots, \text{sim}(\mathbf{z}_x, \mathbf{w}_K)]).$$

This zero-shot formulation enables CLIP to classify unseen categories without fine-tuning but lacks adaptation to the long-tailed and distribution-shifted data in LTSSL.

Out-of-Distribution (OOD) Detection. In the open-world setting of LTSSL, it is essential to detect test samples \mathbf{x} that fall outside the support of the training distribution \mathcal{D}_S , referred to as out-of-distribution (OOD) samples. Given the classifier f trained on \mathcal{D}_S , a common approach to estimate the confidence of a prediction is through the maximum softmax probability (MSP), defined as:

$$\text{MSP}(\mathbf{x}) = \max_{k \in [K]} \frac{e^{f_k(\mathbf{x})}}{\sum_{j=1}^K e^{f_j(\mathbf{x})}}, \quad (1)$$

where $f_k(\mathbf{x})$ denotes the logit corresponding to class k . A lower MSP score typically indicates a higher likelihood that \mathbf{x} is OOD. This simple yet effective criterion enables the model to reject uncertain or unfamiliar inputs that do not align with the long-tailed labeled distribution $\mathbb{P}_S(Y)$ or the test distribution $\mathbb{P}_T(Y)$.

Observation

Experimental setup We conduct experiments using ViT-B/16 (Dosovitskiy et al. 2020) on three long-tailed benchmarks: CIFAR-100-LT, ImageNet-LT, and Places365-LT, with a focus on confidence calibration and OOD detection tasks. To ensure the generalizability of our findings, we adopt both CLIP (Radford et al. 2021) and OpenCLIP () as foundation models, which are pre-trained using different strategies. Prior studies (Shi et al. 2024; Dong et al. 2022) have shown that fine-tuning only a small subset of parameters can yield competitive performance. Building on this insight, we employ AdaptFormer (Chen et al. 2022) as our base parameter-efficient fine-tuning method, combined with the Logit Adjustment criterion. The learning rate, number of training epochs, and parameter initialization settings follow those in (Shi et al. 2024). For comparison, we also train a

model from scratch using CNN-based architectures, following the cRT approach (Kang et al. 2019). Following prior work (Guo et al. 2017), we use Expected Calibration Error (ECE) to evaluate calibration performance. For OOD detection, we report AUC, AP-in, AP-out, and FPR metrics to comprehensively assess models.

Confidence calibration As shown in Fig. 2, we visualize the confidence–accuracy diagram on ImageNet-LT and Places365-LT. Following previous works (Liu et al. 2019), we divide the classes into three groups, “Many”, “Medium”, and “Few”, based on the number of training samples per class. We observe that models trained from scratch tend to exhibit significant overconfidence on the unseen test set, particularly for the tail classes. Specifically, the scratch-trained model yields an ECE of 0.1372 across the entire dataset. Moreover, the tail classes suffer from more pronounced overconfidence compared to head classes. In contrast, models fine-tuned using PEFT demonstrate substantially improved calibration, with tail classes no longer exhibiting such severe overconfidence. We attribute this improvement to the extensive pretraining of foundation models on large-scale data, which reduces model uncertainty and enhances calibration. Additionally, PEFT modifies only a small subset of parameters, thereby preserving the generalization capabilities of the foundation models while effectively adapting to the target task.

OOD detection As shown in Tab. 1, we fine-tune the foundation models on CIFAR-100-LT and evaluate its performance on a variety of OOD datasets, including SVHN (Goodfellow et al. 2013), CIFAR-10 (Krizhevsky, Hinton et al. 2009), Tiny ImageNet (Le and Yang 2015), LSUN (Yu et al. 2015), and Places365 (Zhou et al. 2017). We adopt the MSP as the OOD detection strategy and compare our approach against baseline methods, including OE (Hendrycks, Mazeika, and Dietterich 2018) and OCL (Miao et al. 2024). Across multiple evaluation metrics, the model fine-tuned on OpenCLIP achieves the best overall performance, with an average score of 86.51 across the six datasets. These results demonstrate that our fine-tuned model effectively identifies out-of-distribution samples and generalizes well to diverse OOD scenarios.

Remark Previous experiments show that the fine-tuned model is well calibrated and can effectively detect out-of-distribution samples. These two properties are particularly beneficial for long-tailed semi-supervised learning, where pseudo-labeling confidence and the presence of OOD data pose major challenges. Accurate confidence calibration ensures that the model assigns meaningful probabilities, reducing the risk of incorporating noisy pseudo-labels, especially for tail classes. Meanwhile, robust OOD detection allows the model to filter irrelevant samples from the unlabeled set, preventing harmful supervision signals. Together, these capabilities enhance the reliability and generalization of the model under long-tailed and open-world settings, laying a solid foundation for more effective LTSSL learning.

OOD Dataset	Method	AUC↑	AP-in↑	AP-out↑	FPR↓
Texture	OE	76.01	85.28	57.47	87.45
	OCL	75.92	82.99	66.48	70.01
	PEFT [†]	87.86	92.79	80.15	49.45
	PEFT [‡]	91.32	94.66	86.22	38.26
SVHN	OE	81.82	73.25	89.10	80.98
	OCL	78.64	69.21	86.26	86.38
	PEFT [†]	<u>86.62</u>	<u>73.87</u>	<u>94.26</u>	47.29
	PEFT [‡]	90.68	81.80	95.98	41.00
CIFAR-10	OE	62.60	66.16	57.77	93.53
	OCL	60.29	63.21	55.71	94.22
	PEFT [†]	<u>83.97</u>	<u>84.42</u>	<u>82.61</u>	61.98
	PEFT [‡]	86.39	86.95	85.38	57.38
Tiny ImageNet	OE	68.22	79.36	51.82	88.54
	OCL	69.56	79.97	54.47	85.91
	PEFT [†]	<u>81.34</u>	<u>88.30</u>	<u>70.20</u>	<u>70.03</u>
	PEFT [‡]	83.35	89.85	72.98	66.02
LSUN	OE	76.81	85.33	60.94	83.79
	OCL	<u>79.14</u>	<u>86.56</u>	<u>66.58</u>	<u>75.07</u>
	PEFT [†]	78.16	86.32	65.86	75.45
	PEFT [‡]	81.29	88.45	70.49	69.50
Place365	OE	75.68	60.99	86.51	83.55
	OCL	77.81	62.80	88.39	79.97
	PEFT [†]	<u>84.65</u>	<u>71.67</u>	<u>93.00</u>	<u>58.36</u>
	PEFT [‡]	86.04	74.25	93.65	55.43
Average	OE	73.52	75.06	67.27	86.30
	OCL	73.56	74.12	69.65	81.93
	PEFT [†]	<u>83.77</u>	<u>82.90</u>	<u>81.01</u>	<u>60.43</u>
	PEFT [‡]	86.51	85.99	84.12	54.60

Table 1: The results on OOD tasks on different datasets. PEFT[†] and PEFT[‡] denote the fine-tuned model from CLIP and OpenCLIP, respectively.

Method

LoFT

In modern LTSSL, models are typically optimized by jointly minimizing a supervised classification loss on labeled data, used to learn initial discriminative representations, and a regularization loss on unlabeled data, which further refines the learned features and enhances generalization.

For the supervised classification loss, we adopt the Logit Adjustment (Menon et al. 2020) as the criterion on the labeled long-tailed dataset. The optimization objective is:

$$\mathcal{L}_s = \frac{1}{|\mathcal{D}_S|} \sum_{\mathbf{x} \sim \mathcal{D}_S} H\left(y_b, f(\mathcal{W}(\mathbf{x})) + \tau \log \mathbb{P}_S(Y)\right), \quad (2)$$

where $\mathcal{W}(\cdot)$ denotes a weak augmentation operation (e.g., random crop or horizontal flip), τ is a scaling hyperparameter, and $\mathbb{P}_S(Y)$ represents the empirical class prior estimated from the labeled dataset.

For the regularization loss on unlabeled samples, we follow the basic principle from prior work (Sohn et al. 2020),

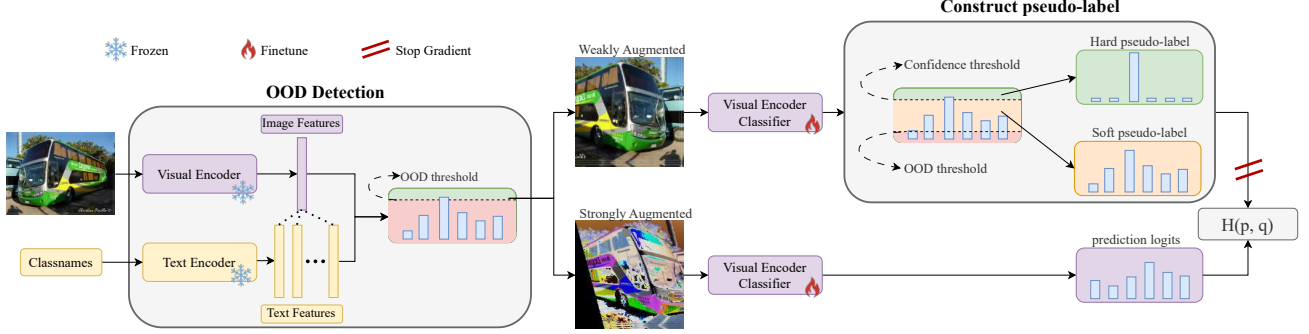


Figure 3: Illustration of the proposed LoFT-OW. $H(p, q)$ denotes the cross-entropy.

where a weakly augmented view is used to generate pseudo-labels, and a strongly augmented view is used to obtain logits for optimization. To better handle uncertain predictions, we partition unlabeled samples into high-confidence and low-confidence subsets based on their Maximum Softmax Probability (MSP), and apply different optimization strategies accordingly. Specifically, we define a binary mask $M_{\mathbf{x}}$ to indicate whether an unlabeled sample is considered high-confidence, computed as:

$$M_{\mathbf{x}} = \begin{cases} 1, & \text{MSP}(\mathbf{x}) > c_u \\ 0, & \text{MSP}(\mathbf{x}) \leq c_u \end{cases} \quad (3)$$

The optimization objective for unlabeled samples is:

$$\begin{aligned} \mathcal{L}_u = \frac{1}{|\mathcal{D}_U|} \sum_{\mathbf{x} \sim \mathcal{D}_U} & \lambda_1 M_{\mathbf{x}} \cdot H(\hat{y}, f(\mathcal{A}(\mathbf{x}))) \\ & + \lambda_2 (1 - M_{\mathbf{x}}) \cdot H(f(\mathcal{W}(\mathbf{x})), f(\mathcal{A}(\mathbf{x}))), \end{aligned} \quad (4)$$

where $\hat{y} = \arg \max f(\mathcal{W}(\mathbf{x}))$ denotes the hard pseudo-label derived from the weakly augmented view, and $\mathcal{A}(\cdot)$ denotes a strong augmentation. λ_1 and λ_2 are hyperparameters.

In Eq. 4, for high-confidence samples ($M_{\mathbf{x}} = 1$), we apply hard pseudo-labels by assigning the most probable class using the model's prediction. For low-confidence samples ($M_{\mathbf{x}} = 0$), we apply soft pseudo-labels by leveraging the full predicted probability distribution, which provides smoother supervision and better captures prediction uncertainty. We analyze that, as shown in Fig. 2, under our fine-tuning framework, the model's confidence score is strongly correlated with prediction accuracy. Since high-confidence samples are generally more reliable, we apply hard supervision to them, while soft supervision is used for low-confidence samples to mitigate overfitting and enhance generalization. Furthermore, as discussed previously, our fine-tuned model exhibits better calibration for tail classes compared to models trained from scratch. Consequently, we do not distinguish between head and tail classes when determining the confidence mask in Eq. 3, e.g., setting different thresholds for head or tail classes, which also reduces the number of required hyper-parameters. Finally, the overall training objective is:

$$\mathcal{L} = \mathcal{L}_s + \mathcal{L}_u \quad (5)$$

LoFT-OW (LoFT under Open-World scenarios)

Traditional LTSSL methods typically assume that all unlabeled data originates from the same distribution as the labeled data—a condition that rarely holds in real-world scenarios. In practice, unlabeled data are often collected from broad, unconstrained sources such as the web or dynamic field environments, where it is highly likely that a substantial portion of samples lie outside the distribution of the pre-defined labeled classes. These OOD samples, if not properly handled, can degrade model performance by introducing misleading supervision. To address this challenge, we propose an extension of our framework to open-world settings, termed LoFT-OW (LoFT under Open-World scenarios). LoFT-OW is designed to effectively detect and filter out OOD samples during training, thereby mitigating their adverse effects and enhancing performance in long-tailed, semi-supervised learning.

As shown in Fig. 3, we adopt a two-stage filtering strategy to identify out-of-distribution (OOD) samples. In the first stage, we employ a zero-shot filtering mechanism, where the foundation model assigns confidence scores to each unlabeled sample. Only those with confidence exceeding a high-confidence threshold t_{HC} are retained, resulting in a cleaner and more reliable pseudo-labeled subset, denoted as $\tilde{\mathcal{D}}_U$. This filtered dataset is typically smaller in size and can be leveraged for subsequent fine-tuning. Beyond this initial stage, we further exploit the strong OOD detection capability of the fine-tuned model, which has been verified previously. We define the filtering function as follows:

$$M_{\mathbf{x}}^{ood} = \begin{cases} 1, & \text{MSP}(\mathbf{x}) > c_{ood} \\ 0, & \text{MSP}(\mathbf{x}) \leq c_{ood} \end{cases}, \quad (6)$$

where c_{ood} is the hyper-parameter to control the filtering strength. Then the optimization object for the unlabeled set under open-world scenarios is:

$$\begin{aligned} \mathcal{L}_u = \frac{1}{|\tilde{\mathcal{D}}_U|} \sum_{\mathbf{x} \sim \tilde{\mathcal{D}}_U} & \lambda_1 M_{\mathbf{x}}^{ood} M_{\mathbf{x}} \cdot H(\hat{y}, f(\mathcal{A}(\mathbf{x}))) \\ & + \lambda_2 M_{\mathbf{x}}^{ood} (1 - M_{\mathbf{x}}) \cdot H(f(\mathcal{W}(\mathbf{x})), f(\mathcal{A}(\mathbf{x}))), \end{aligned} \quad (7)$$

CIFAR-100-LT									
Method	$\gamma = \gamma_l = \gamma_u = 10$				$\gamma = \gamma_l = \gamma_u = 20$		$\gamma_u = 1$ (uniform)		$\gamma_u = 1/10$ (reversed)
	$N_1 = 50$	$N_1 = 150$	$N_1 = 50$	$N_1 = 150$	$N_1 = 50$	$N_1 = 150$	$N_1 = 50$	$N_1 = 150$	
FixMatch	45.2	56.5	40.0	50.7	45.5	58.1	44.2	57.3	
+ACR	55.7	65.6	48.0	58.9	66.0	73.4	57.0	67.6	
+ACR+BEM	55.8	66.3	48.6	59.8	-	-	-	-	
+TCBC	-	59.4	-	53.9	-	63.2	-	59.9	
+CPE	50.3	59.8	43.8	55.6	-	-	-	60.8	
+CCL	53.5	63.5	46.8	57.5	59.8	67.9	54.4	64.7	
CLIP	PEFT	75.5	79.7	74.0	78.4	75.5	79.7	75.5	79.7
	LoFT	78.8	81.1	75.3	79.3	78.0	81.0	77.3	80.6
	LoFT-OW	76.5	79.9	73.6	78.6	76.6	80.0	76.4	80.0
OpenCLIP	PEFT	78.0	81.7	75.3	81.1	78.0	81.7	78.0	81.7
	LoFT	81.8	83.2	78.4	81.2	80.3	83.6	79.8	82.3
	LoFT-OW	79.3	81.6	75.4	80.8	78.6	82.1	79.7	82.0

Table 2: The results on CIFAR-100-LT with different hyper-parameters of γ_u and γ_l .

Method	training iterations	Accuracy
FixMatch	250000	42.3
+BEM	250000	58.2
+ACR	250000	63.6
+ACR+BEM	250000	63.9
+CCL	250000	67.8
CLIP	PEFT	10000
	LoFT	10000
	LoFT-OW	10000
OpenCLIP	PEFT	10000
	LoFT	10000
	LoFT-OW	10000

Table 3: The results on ImageNet-127.

Experiments

Experimental Setup

To validate the efficacy of our method under long-tailed distributions and in open-world semi-supervised learning scenarios, we conduct experiments on two long-tailed benchmarks: CIFAR-100-LT (Cui et al. 2019), ImageNet-127 (Wei et al. 2021). For ImageNet-127, we only use 1% of the unlabeled data compared with ACR. For CIFAR-100-LT, let N_k denote the number of labeled samples for class k , with $N_1 \geq N_2 \geq \dots \geq N_K$. The imbalance ratio of the labeled dataset is defined as $\gamma_l = \frac{N_1}{N_C}$. Similarly, let M_c denote the number of unlabeled samples for class c , and the imbalance ratio of the unlabeled dataset is defined as $\gamma_u = \frac{\max_c M_c}{\min_c M_c}$, without assuming any specific class distribution. We consider three representative settings:

- Consistent: $M_1 \geq M_2 \geq \dots \geq M_C$ with $\gamma_u = \gamma_l$.
- Uniform: $M_1 = M_2 = \dots = M_C$, i.e., $\gamma_u = 1$.
- Reversed: $M_1 \leq M_2 \leq \dots \leq M_C$, i.e., $\gamma_u = 1/\gamma_l$.

- Reversed: $M_1 \leq M_2 \leq \dots \leq M_C$, i.e., $\gamma_u = 1/\gamma_l$.

To simulate the open-world setting, we introduce the COCO (Lin et al. 2014) dataset as OOD source. COCO contains a diverse set of object categories that are semantically disjoint from those in the target classification task, making it a suitable candidate for evaluating OOD robustness. We mix the COCO dataset with the current unlabeled set to form a more realistic and challenging unlabeled pool, which better reflects the distributional uncertainty encountered in open-world scenarios. We set $t_{HC} = 0.95$ for all datasets.

We compare LoFT and LoFT-OW with FixMatch (Sohn et al. 2020), as well as equipped with different methods, ACR (Wei and Gan 2023), ACR+BEM (Zheng et al. 2024), TCBC (Li et al. 2024), CPE (Ma et al. 2024), and CCL (Zhou et al. 2024). All experiments are performed on a single NVIDIA A40 GPU. More dataset introduction and hyper-parameter of our method are in the Appendix.

Results on LoFT

CIFAR-100-LT As shown in Tab. 2, LoFT consistently outperforms PEFT across all settings on CIFAR-100-LT, using both CLIP and OpenCLIP backbones. With OpenCLIP, LoFT achieves the best results in all cases (up to 83.2%), demonstrating its effectiveness. In terms of imbalance levels, LoFT performs well under all γ values. Performance slightly decreases as γ increases (e.g., from $\gamma = 10$ to $\gamma = 20$), indicating increased difficulty with more severe imbalance, but LoFT still maintains a clear margin over PEFT. Moreover, LoFT remains robust under uniform and reversed unlabeled distributions ($\gamma_u = 1$ and $1/10$), further validating its ability to handle various class distributions.

ImageNet-127 As shown in Tab. 3, our method outperforms other methods on a large-scale long-tailed dataset, demonstrating the strong generalization ability of LoFT.



Figure 4: Visualizations of unlabeled samples and their predicted confidence scores on ImageNet-127. Samples with a green background are assigned reliable pseudo-labels with high confidence, while the sample with a red background is identified as an OOD instance.

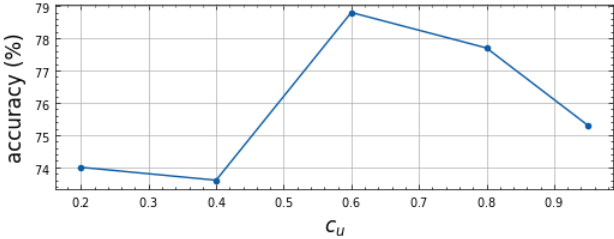


Figure 5: Ablation studies on hyper-parameter c_u . The horizontal axis represents the value of c_u , and the vertical axis represents the accuracy.

Compared to PEFT, LoFT consistently achieves higher accuracy with both CLIP and OpenCLIP backbones, reaching 73.3% and 73.9%, respectively. These improvements over strong baselines and prior methods (e.g., FixMatch+CCL at 67.8%) highlight LoFT’s effectiveness beyond small-scale datasets, confirming its robustness and scalability in real-world, large-scale long-tailed semi-supervised learning scenarios. Moreover, we visualize the unlabeled samples and their prediction scores, as shown in Fig. 4. For samples containing meaningful content within the label space, LoFT-OW generates reliable pseudo-labels. In contrast, for uninformative OOD samples, LoFT-OW assigns low confidence scores, facilitating their detection.

Results on LoFT-OW

As shown in Tab. 2 and Tab. 3, LoFT-OW achieves strong performance on both CIFAR-100-LT and ImageNet-127, with fewer training iterations and less data. While its accuracy on CIFAR-100-LT is slightly lower than LoFT due to the inclusion of OOD unlabeled data, which introduces distributional shifts and may hinder representation learning, LoFT-OW remains competitive across all imbalance settings. Notably, on the larger and more complex ImageNet-127 dataset, LoFT-OW outperforms all baselines, including LoFT, demonstrating its superior scalability. This highlights the effectiveness of LoFT-OW in leveraging OOD data when generalizing to more diverse and large-scale benchmarks.

Ablation studies

We perform two ablation experiments on the CIFAR-100-LT benchmark ($N = 50$, $M = 400$, imbalance ratio = 10), using CLIP as our foundation model.

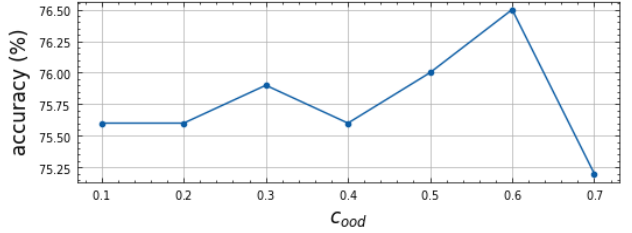


Figure 6: Ablation studies on hyper-parameter c_{oob} . The horizontal axis represents the value of c_{oob} , and the vertical axis represents the accuracy.

Effect of the hyper-parameter c_u The hyper-parameter c_u controls the balance between hard and soft pseudo-label assignments. With a large value of c_u , more unlabeled samples are assigned hard pseudo-labels, encouraging confident and deterministic supervision but potentially introducing noise if the predictions are incorrect. In contrast, a smaller value of c_u leads to a greater proportion of soft pseudo-labels, which provides more nuanced guidance by preserving model uncertainty, thereby reducing the risk of reinforcing incorrect predictions. As shown in Fig. 5, the test accuracy rises from 74.0% at $c_u = 0.2$ to a maximum of 78.8% at $c_u = 0.6$, then gradually declines to 75.3% at $c_u = 0.95$. This behavior indicates that a moderate confidence cutoff best balances the benefit of incorporating pseudo-labels with the risk of introducing erroneous predictions.

Effect of the hyper-parameter c_{oob} The hyper-parameter c_{oob} controls the sensitivity of OOD detection among unlabeled samples. A larger value of c_{oob} enforces stricter filtering, ensuring higher quality among the retained samples but resulting in fewer valid pseudo-labeled instances. Conversely, a smaller c_{oob} allows more samples to pass the filter, increasing quantity but potentially compromising quality due to the inclusion of OOD data. Fig. 6 shows that accuracy improves from 75.6% at $c_{oob} = 0.1$ to 76.5% at $c_{oob} = 0.6$ before falling to 75.2% at $c_{oob} = 0.7$. These results suggest that a moderate OOD cutoff effectively excludes out-of-distribution samples without discarding too much valuable unlabeled data. Combined with previous experiments, both c_u and c_{oob} present the optimal result at the value of 0.6. In the standard LTSSL scenario, $c_u = 0.6$ corresponds to a confidence level high enough to regard predictions as reliable pseudo-labels. In the open-world setting, $c_{oob} = 0.6$ similarly acts as a boundary above which samples are very likely to be in-distribution, thus improving data filtering.

Conclusion

In this work, we revisit LTSSL and propose LoFT, a parameter-efficient framework built on transformer-based foundation models. LoFT tackles key LTSSL challenges such as overconfidence, poor early pseudo-labels, and tail class inefficiency. Leveraging pre-trained models, it enhances calibration, reduces training overhead, and improves pseudo-label quality. We further extend LTSSL to open-world settings with LoFT-OW, which incorporates OOD detection to filter irrelevant samples. Extensive experiments

show that LoFT performs competitively in both standard and open-world LTSSL, offering a practical solution for real-world imbalanced learning.

References

Chen, S.; Ge, C.; Tong, Z.; Wang, J.; Song, Y.; Wang, J.; and Luo, P. 2022. Adaptformer: Adapting vision transformers for scalable visual recognition. *Advances in Neural Information Processing Systems*, 35: 16664–16678.

Cui, Y.; Jia, M.; Lin, T.-Y.; Song, Y.; and Belongie, S. 2019. Class-balanced loss based on effective number of samples. In *Proceedings of the IEEE Conference on Computer Vision and Pattern Recognition*, 9268–9277.

Dong, B.; Zhou, P.; Yan, S.; and Zuo, W. 2022. Lpt: Long-tailed prompt tuning for image classification. *arXiv preprint arXiv:2210.01033*.

Dosovitskiy, A.; Beyer, L.; Kolesnikov, A.; Weissenborn, D.; Zhai, X.; Unterthiner, T.; Dehghani, M.; Minderer, M.; Heigold, G.; Gelly, S.; et al. 2020. An image is worth 16x16 words: Transformers for image recognition at scale. *arXiv preprint arXiv:2010.11929*.

Goodfellow, I. J.; Bulatov, Y.; Ibarz, J.; Arnoud, S.; and Shet, V. 2013. Multi-digit number recognition from street view imagery using deep convolutional neural networks. *arXiv preprint arXiv:1312.6082*.

Guo, C.; Pleiss, G.; Sun, Y.; and Weinberger, K. Q. 2017. On calibration of modern neural networks. In *International conference on machine learning*, 1321–1330. PMLR.

Hendrycks, D.; and Gimpel, K. 2016. A baseline for detecting misclassified and out-of-distribution examples in neural networks. *arXiv preprint arXiv:1610.02136*.

Hendrycks, D.; Mazeika, M.; and Dietterich, T. 2018. Deep anomaly detection with outlier exposure. *arXiv preprint arXiv:1812.04606*.

Hou, Y.; and Jia, Y. 2025. A Square Peg in a Square Hole: Meta-Expert for Long-Tailed Semi-Supervised Learning. *arXiv preprint arXiv:2505.16341*.

Kang, B.; Xie, S.; Rohrbach, M.; Yan, Z.; Gordo, A.; Feng, J.; and Kalantidis, Y. 2019. Decoupling representation and classifier for long-tailed recognition. *arXiv preprint arXiv:1910.09217*.

Krizhevsky, A.; Hinton, G.; et al. 2009. Learning multiple layers of features from tiny images.

Le, Y.; and Yang, X. 2015. Tiny imagenet visual recognition challenge. *CS 231N*, 7(7): 3.

Li, L.; Tao, B.; Han, L.; Zhan, D.-c.; and Ye, H.-j. 2024. Twice class bias correction for imbalanced semi-supervised learning. In *Proceedings of the AAAI Conference on Artificial Intelligence*, volume 38, 13563–13571.

Lin, T.-Y.; Maire, M.; Belongie, S.; Hays, J.; Perona, P.; Ramanan, D.; Dollár, P.; and Zitnick, C. L. 2014. Microsoft coco: Common objects in context. In *European conference on computer vision*, 740–755. Springer.

Liu, K.; Fu, Z.; Jin, S.; Chen, C.; Chen, Z.; Jiang, R.; Zhou, F.; Chen, Y.; and Ye, J. 2024. Rethinking out-of-distribution detection on imbalanced data distribution. *Advances in Neural Information Processing Systems*, 37: 109152–109176.

Liu, Z.; Miao, Z.; Zhan, X.; Wang, J.; Gong, B.; and Yu, S. X. 2019. Large-scale long-tailed recognition in an open world. In *Proceedings of the IEEE Conference on Computer Vision and Pattern Recognition*, 2537–2546.

Ma, C.; Elezi, I.; Deng, J.; Dong, W.; and Xu, C. 2024. Three heads are better than one: Complementary experts for long-tailed semi-supervised learning. In *Proceedings of the AAAI Conference on Artificial Intelligence*, volume 38, 14229–14237.

Menon, A. K.; Jayasumana, S.; Rawat, A. S.; Jain, H.; Veit, A.; and Kumar, S. 2020. Long-tail learning via logit adjustment. *arXiv preprint arXiv:2007.07314*.

Miao, W.; Pang, G.; Bai, X.; Li, T.; and Zheng, J. 2024. Out-of-distribution detection in long-tailed recognition with calibrated outlier class learning. In *Proceedings of the AAAI Conference on Artificial Intelligence*, volume 38, 4216–4224.

Ouali, Y.; Hudelot, C.; and Tami, M. 2020. An overview of deep semi-supervised learning. *arXiv preprint arXiv:2006.05278*.

Peng, H.; Pian, W.; Sun, M.; and Li, P. 2023. Dynamic re-weighting for long-tailed semi-supervised learning. In *Proceedings of the IEEE/CVF winter conference on applications of computer vision*, 6464–6474.

Radford, A.; Kim, J. W.; Hallacy, C.; Ramesh, A.; Goh, G.; Agarwal, S.; Sastry, G.; Askell, A.; Mishkin, P.; Clark, J.; et al. 2021. Learning transferable visual models from natural language supervision. In *International conference on machine learning*, 8748–8763. PMLR.

Sanchez Aimar, E.; Jonnarth, A.; Felsberg, M.; and Kuhlmann, M. 2023. Balanced Product of Calibrated Experts for Long-Tailed Recognition. In *Proceedings of the IEEE/CVF Conference on Computer Vision and Pattern Recognition (CVPR)*, 19967–19977.

Shi, J.-X.; Wei, T.; Zhou, Z.; Shao, J.-J.; Han, X.-Y.; and Li, Y.-F. 2024. Long-Tail Learning with Foundation Model: Heavy Fine-Tuning Hurts. In *Forty-first International Conference on Machine Learning*.

Sohn, K.; Berthelot, D.; Carlini, N.; Zhang, Z.; Zhang, H.; Raffel, C. A.; Cubuk, E. D.; Kurakin, A.; and Li, C.-L. 2020. Fixmatch: Simplifying semi-supervised learning with consistency and confidence. *Advances in neural information processing systems*, 33: 596–608.

Tian, C.; Wang, W.; Zhu, X.; Dai, J.; and Qiao, Y. 2022. Vilt: Learning class-wise visual-linguistic representation for long-tailed visual recognition. In *European Conference on Computer Vision*, 73–91. Springer.

Tomaní, C.; Gruber, S.; Erdem, M. E.; Cremers, D.; and Buettner, F. 2021. Post-Hoc Uncertainty Calibration for Domain Drift Scenarios. In *Proceedings of the IEEE/CVF Conference on Computer Vision and Pattern Recognition (CVPR)*, 10124–10132.

Wei, C.; Sohn, K.; Mellina, C.; Yuille, A.; and Yang, F. 2021. Crest: A class-rebalancing self-training framework

for imbalanced semi-supervised learning. In *Proceedings of the IEEE/CVF conference on computer vision and pattern recognition*, 10857–10866.

Wei, T.; and Gan, K. 2023. Towards Realistic Long-Tailed Semi-Supervised Learning: Consistency Is All You Need. In *Proceedings of the IEEE/CVF Conference on Computer Vision and Pattern Recognition (CVPR)*, 3469–3478.

Xu, Z.; Chai, Z.; and Yuan, C. 2021. Towards calibrated model for long-tailed visual recognition from prior perspective. *Advances in Neural Information Processing Systems*, 34: 7139–7152.

Yu, F.; Seff, A.; Zhang, Y.; Song, S.; Funkhouser, T.; and Xiao, J. 2015. Lsun: Construction of a large-scale image dataset using deep learning with humans in the loop. *arXiv preprint arXiv:1506.03365*.

Zhang, H.; Cisse, M.; Dauphin, Y. N.; and Lopez-Paz, D. 2017. mixup: Beyond empirical risk minimization. *arXiv preprint arXiv:1710.09412*.

Zheng, H.; Zhou, L.; Li, H.; Su, J.; Wei, X.; and Xu, X. 2024. Bem: Balanced and entropy-based mix for long-tailed semi-supervised learning. In *Proceedings of the IEEE/CVF Conference on Computer Vision and Pattern Recognition*, 22893–22903.

Zhong, Z.; Cui, J.; Liu, S.; and Jia, J. 2021. Improving calibration for long-tailed recognition. In *Proceedings of the IEEE/CVF conference on computer vision and pattern recognition*, 16489–16498.

Zhou, B.; Lapedriza, A.; Khosla, A.; Oliva, A.; and Torralba, A. 2017. Places: A 10 million Image Database for Scene Recognition. *IEEE Transactions on Pattern Analysis and Machine Intelligence*.

Zhou, Z.-H.; Fang, S.; Zhou, Z.-J.; Wei, T.; Wan, Y.; and Zhang, M.-L. 2024. Continuous contrastive learning for long-tailed semi-supervised recognition. *Advances in Neural Information Processing Systems*, 37: 51411–51435.